IChemE

www.icheme.org/journals
doi: 10.1205/cherd.03238

0263–8762/05/$30.00+0.00

Trans IChemE, Part A, September 2005
Chemical Engineering Research and Design, 83(A9): 1103–1110

EXPERIMENTAL STUDY ON THE TRANSITION IN THE VELOCITY OF INDIVIDUAL TAYLOR BUBBLES IN VERTICAL UPWARD CO-CURRENT LIQUID FLOW

A. M. F. R. PINTO[1]*, M. N. COELHO PINHEIRO[2], S. NOGUEIRA[1,3], V. D. FERREIRA[1] and J. B. L. M. CAMPOS[1]

[1]*Centro de Estudos de Fenómenos de Transporte, Departamento de Eng. Química, Faculdade de Engenharia da Universidade do Porto, Porto—Portugal*
[2]*Departamento de Engenharia Química, Instituto Superior de Engenharia de Coimbra, Coimbra, Portugal*
[3]*von Karman Institute for Fluid Dynamics, Rhode Saint Genèse, Belgium*

An experimental study is presented concerning the transition in the velocity of individual Taylor bubbles in vertical co-current liquid flow. Velocities of individual Taylor bubbles rising in co-current liquids (kinematic viscosities from 10^{-6} to $5.7 \times 10^{-6}\ m^2\ s^{-1}$) in acrylic columns of 22 mm, 32 mm and 52 mm internal diameter were measured for a wide range of Reynolds number of the flowing liquid using two non-intrusive experimental techniques. The measuring section was located at 6.0 m from the gas injection. The operating conditions used correspond to inertial controlled regime. The data showed an unexpected feature of the bubble motion: the velocity coefficient C changes even when the flow regime in the liquid ahead the bubble is still laminar, i.e., the transition in the bubble velocity starts at liquid Reynolds numbers much lower than 2100. Additional experiments, employing PIV measurements, showed a developed laminar liquid flow ahead the bubble nose. Based on a dimensional analysis, the most important dimensionless numbers for the phenomena were identified and, after processing all data, an empirical correlation was established to predict the velocity coefficient C for a large range of operation conditions. This information is very important for vertical two-phase slug flow modelling.

Keywords: two-phase flow; slug flow regime; Taylor bubble velocity.

INTRODUCTION

Slug flow is a very common occurrence in gas–liquid two-phase flow over a wide range of flow parameters (gas and liquid flow rates and pipe diameters) and is found in a variety of industrial applications. In particular, predictive modelling of slug flow is used by the hydrocarbon recovery industry, to optimize the design and operation of sub-sea multiphase hydrocarbon pipelines.

Slug flow is characterized by a chaotic alternation of liquid slugs and long bullet-shaped bubbles (Taylor bubbles) almost filling the pipe cross-section. Between the bubbles and the pipe wall flows a thin liquid film. Because of its imminent unsteadiness, the slug flow pattern is highly complex and extremely difficult to predict. There is a need of experimental studies providing experimental data to built predictive models. In particular, information about the Taylor bubble velocity is essential to the development of these models.

The rise of a single elongated bubble, in stagnant and in flowing liquid in a vertical pipe, has been extensively studied. Collins *et al.* (1978) presented a theory describing the motion of a Taylor bubble rising through upward flowing liquid in a vertical pipe. They presented solutions for both laminar and turbulent liquid regimes. The comparison between predictions and experiments was excellent for the turbulent case but for the laminar one, the data were in reasonable agreement with experiments only at low liquid velocities. The authors attributed this discrepancy to the undeveloped laminar liquid flow at the measuring section. Fréchou (1986) experimentally confirmed the turbulent model presented by Collins *et al.* (1978) and observed that the transition for the Taylor bubble velocity started at liquid Reynolds numbers lower than expected. Mao and Dukler (1991) obtained similar results. These unexpected results were put in evidence in the review work of Fabre and Liné (1992). Nowadays, there are still, in the literature, some doubts concerning the transition for the Taylor bubble velocity which has a strong influence on

*Correspondence to: Dr A. M. F. R. Pinto, Centro de Estudos de Fenómenos de Transporte, Departamento de Eng. Química, Faculdade de Engenharia da Universidade do Porto, Rua Dr. Roberto Frias, 4200-465, Porto, Portugal. E-mail: apinto@fe.up.pt

the dynamics of slug flow. This topic was extensively investigated in the present work.

PREVIOUS WORK

Following Nicklin *et al.* (1962), the velocity of an individual Taylor bubble rising in a flowing liquid, U, is represented as a sum of two terms:

$$U = CU_L + U_\infty \tag{1}$$

where U_∞ is the bubble velocity in a stagnant fluid and U_L the average liquid velocity.

According to White and Beardmore (1962) and Zukoski (1966), U_∞ is a function of g, the acceleration due to gravity, D, the internal tube diameter, and ρ, μ, and σ, respectively, density, viscosity and surface tension of the liquid. From the dimensional analysis it follows that the Froude number, $Fr = U_\infty/(gD)^{1/2}$ is a unique function of the dimensionless inverse viscosity number, $N_f = g^{1/2}D^{3/2}\rho/\mu$ and of the Morton number, $M = g\mu^4/\rho\sigma^3$. For sufficiently large tubes, the bubble rising velocity in stagnant liquids of low and moderate viscosity, is independent of liquid properties and so Fr is independent of N_f and M. According to Collins *et al.* (1978) this inertial controlled regime is specified by $N_f > 300$ and $N_f^{4/3}M^{1/3} > 100$ and White and Beardmore (1962) and Stewart and Davidson (1967) suggested $Fr = 0.35$ for this regime.

Collins *et al.* (1978) studied the motion of a Taylor bubble rising through an upward flowing liquid and presented solutions to both, laminar and turbulent liquid flows, in the form

$$U = U_C + (gD)^{1/2}\phi\left\{\frac{U_C}{(gD)^{1/2}}\right\} \tag{2}$$

where U_C is the liquid velocity at the tube axis and ϕ indicates a functional relationship, which depends upon the shape of the liquid velocity profile ahead of the bubble. They assumed potential axisymmetric flow and solved the Stoke's stream function equation with the appropriate boundary conditions at the bubble surface. The authors showed that for a turbulent liquid flow, the bubble velocity is well predicted by

$$U = U_L\left(\frac{\ln Re_{U_L} + 0.089}{\ln Re_{U_L} - 0.74}\right) + 0.347(gD)^{1/2} \times \phi\left\{\frac{U_L}{(gD)^{1/2}}\frac{1.81}{\ln Re_{U_L} - 0.74}\right\} \tag{3}$$

where Re_{U_L} is the Reynolds number of the flowing liquid (with mean velocity U_L). The coefficient of U_L (right side, first term) expresses the dependence of U_C/U_L on Re_{U_L}. There is an excellent agreement between these results and Nicklin's equation with $C = 1.20$. The coefficient 1.20 is close to the ratio $C = U_C/U_L = 1.22$ obtained from a one seventh power-law velocity profile. The laminar solution obtained by Collins *et al.* (1978) was

$$U = 2.0\,U_L + 0.347(gD)^{1/2} \times \phi\left\{\frac{2.39U_L}{(gD)^{1/2}}\right\} \tag{4}$$

The comparison of these results and Nicklin's equation with $C = 2.0$ gives a quite good agreement. The coefficient 2.0 is equal to the ratio $C = U_C/U_L = 2.0$ obtained from a parabolic laminar profile.

Collins *et al.* (1978) experimentally confirmed the theoretical predictions for turbulent flow, but in the laminar case the agreement was only achieved for low values of U_L. The authors explained the deviations by means of pipe entrance effects, which induced an undeveloped profile at the measuring section. The ratio, between the entry length and the pipe diameter, is proportional to Re_{U_L}, the constant of proportionality being quoted as 0.08 (theoretical, White, 1974), or 0.028 (experimental, Govier and Aziz, 1972).

Other investigators (Polonsky *et al.*, 1998) observed similar deviations from theoretical predictions. Also, several published papers on the motion of a train of elongated bubbles in slug flow (Fréchou, 1986; Mao and Dukler, 1991), suggest that when the Reynolds number of the mixture decreases below some critical value, laminar flow is expected and the bubble velocity should increase. However, their results showed that the liquid Reynolds numbers, for which the transition occurs, are lower than expected. The authors tried to explain their results by the occurrence of turbulence in the falling film flowing around long Taylor bubbles and also by the propagation of rippling waves along this falling film.

In the present work, the velocity coefficient C was determined for a wide range of operation conditions in inertial controlled regime, using two non-intrusive techniques, allowing the identification of the critical transition zones for the bubble velocity. A general correlation was established to predict C over the whole conditions range.

PROCEDURE AND EXPERIMENTAL CONDITIONS

The bubble velocity was followed by means of two experimental techniques.

- One technique is based on the signals of differential pressure transducers connected to the vertical pipe at 6.0 m from the gas injection. Pinto and Campos (1996) and Pinto *et al.* (1998) carefully described the basis of this experimental method. The signals from the transducers (T_1 and T_2 in Figure 1) were acquired at a frequency of 250 Hz by a computer with an analog–digital board and recorded for later processing, after conversion into pressure data. For each experimental condition, six to 10 acquisitions of the transducers signals were performed. The corresponding bubble velocity was obtained from the mean of the velocity values, after analysis of the recorded pressure files. Only velocity values with a deviation from the mean value lower than 3% were considered.
- The bubble velocity was also measured by means of a second technique comprising two laser diodes placed close to the column, pointing to two photocells placed in the opposite side of the column but slightly deviated from the central plane (around 1 mm). The presence of the bubble causes a deflection of the laser beams and the photocells signals (converted to voltage) drop abruptly (Figure 1). The analysis of signals and the distance between photocells were used to compute the

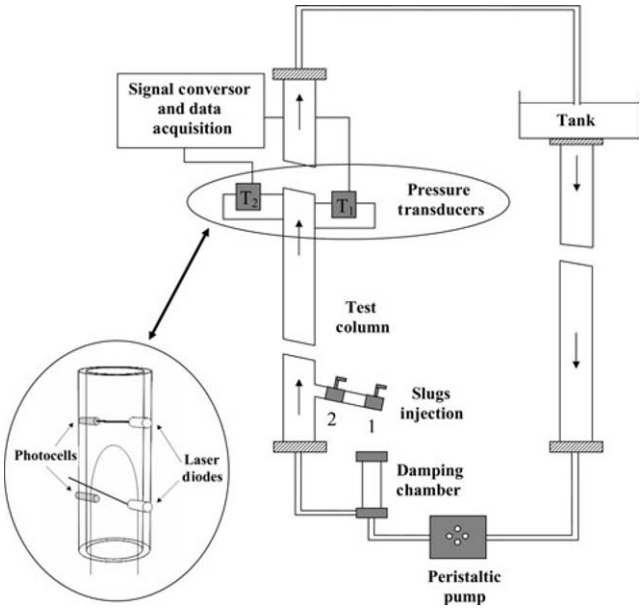

Figure 1. Experimental set-up with representation of the two techniques used to measure the Taylor bubble velocity.

bubble velocity. Two pairs of laser diodes/photocells placed upper 6.0 m from the gas injection, enabled the determination, for each studied condition, of the mean bubble velocity. For some selected operation conditions, as will be explained in the next section, the velocity profiles ahead of the bubble were determined. A simultaneous PIV (particle image velocimetry) and Shadowgraphy technique recently developed and implemented, was used as described in detail by Nogueira *et al.* (2003).

The experimental set-up used in this study is sketched in Figure 1. The experiments were performed in acrylic columns with 22 mm, 32 mm and 52 mm internal diameter and a peristaltic pump with variable speed was used to control the liquid flow rate. In order to maintain a continuous flow rate in the test column, a damping chamber was placed between the pump outlet and the column. To measure the liquid flow rate, a plastic hose dipped into the liquid inside the tank was drained and the volume collected in a graduated container was measured over a period of time. Several measurements were performed to ensure reproducibility. A wide range of mean liquid velocities (8.59×10^{-3} to 1.44×10^{-1} m s^{-1} in the larger column and 2.47×10^{-3} to 5.92×10^{-1} m s^{-1} in the narrower column) was covered.

Near the bottom of the test column there was a mechanism for bubble injection, sketched also in Figure 1. The bubble was released by manipulating the two ball valves. Initially, with valve 1 open and valve 2 closed, the space between valves was filled with air. The Taylor bubble was released into the test column by closing valve 1 and opening valve 2. The volume of gas injected into the column was enough to generate a long Taylor bubble with a stabilized liquid film (Campos and Guedes de Carvalho, 1988).

Water and aqueous glycerol solutions with a wide range of kinematic viscosities (10^{-6} to 5.7×10^{-6} m^2 s^{-1}) were used. Special care was required to maintain nearly uniform the temperature of the liquid inside the column. The liquid viscosity at the different values of temperature registered during the experiments was measured with a Brookfield rotating viscometer.

The liquid densities were measured and the surface tension values were estimated using data from White and Beardmore (1962).

The physical properties of the liquids used in the experiments are summarised in Table 1 with some other parameters of interest. The temperature values indicated in Table 1 correspond to the average of the values registered during the set of experiments performed with a given solution. In the next section all the data shown will be processed with the physical properties estimated or measured at the registered values of temperature.

Experiments with a single bubble rising through the quiescent liquid, with a ball valve either closed or opened at the top of the test column, were also performed. The aim of these experiments was to obtain an estimate of the increase in the Taylor bubble velocity due to the bubble expansion during its rise. This estimate was used to correct all the velocity data shown in the next section.

RESULTS AND DISCUSSION

The plots of Figure 2(a)–(c) show the values of the velocity of an isolated Taylor bubble, U, rising in co-current flowing water with velocity U_L, in acrylic columns with 22 mm, 32 mm and 52 mm internal diameter, respectively. In these figures, the full symbols were obtained from the transducer signals and the open symbols from the diode-photocell technique. The values obtained by the different techniques are in very good agreement.

According to equation (1), the correlation between U and U_L is linear. The slope (C) of the straight lines will be about 2.0 for laminar regime in the flowing liquid and 1.2 for turbulent regime. The intercept value (U_∞) will be equal to the velocity of an isolated bubble rising in the tube with no net liquid flow. The full lines in the plots are obtained from equation (1) (valid for inertial controlled regime) with $C = 2.0$ and $C = 1.2$, which are good fits to the experimental data for $Re_{U_L} < 2100$ and $Re_{U_L} > 4000$, respectively. These results show that in the experiments performed in water, the transition in the bubble velocity

Table 1. Physical properties of the liquids used in the experiments.

Liquid	T (°C)	$\mu \times 10^3$ (Pa s)	ρ (kg m^3)	$\sigma \times 10^3$ (N m^{-1})	N_f^a	M
Water	20.3	1.00	1000	72.40	10 215–37 121	2.582×10^{-11}
Glycerol (24% wt)	18.4	2.04	1070	71.02	5964–23 032	5.757×10^{-10}
Glycerol (45% wt)	19.9	4.66	1111	70.29	2377–9738	1.232×10^{-8}
Glycerol (51% wt)	20.1	6.45	1126	69.80	1716–1927	4.637×10^{-8}

[a]The lower values correspond to the narrowest column and the higher to the largest column.

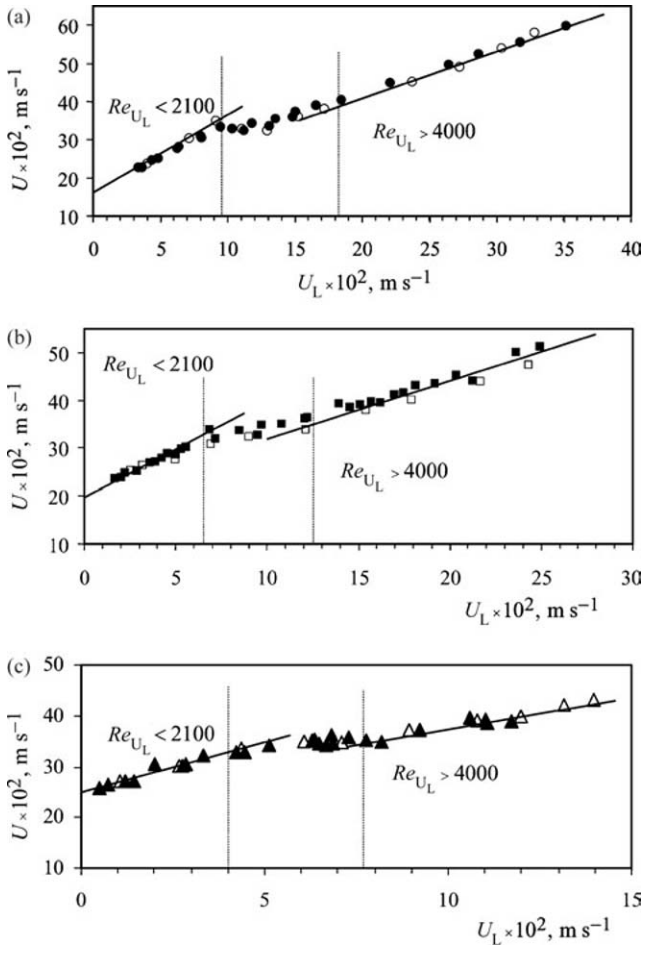

Figure 2. Velocity of an isolated Taylor bubble rising through flowing water in a vertical tube with (a) 22 mm—●, ○; (b) 32 mm—■, □; and (c) 52 mm—▲, △ internal diameter. The open symbols correspond to experiments with the laser diodes/photocells technique.

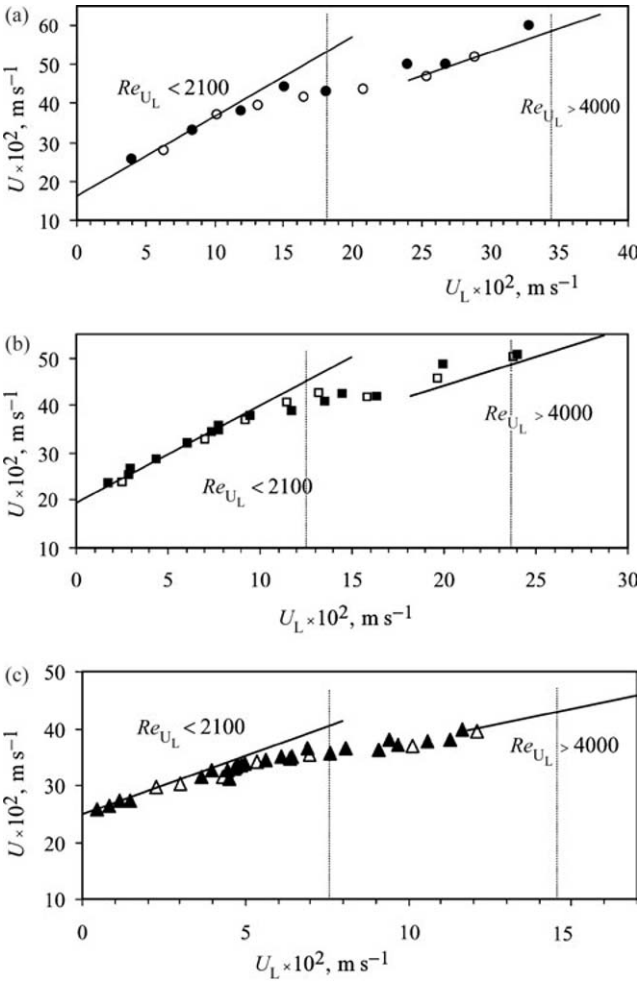

Figure 3. Velocity of an isolated Taylor bubble rising through a glycerol solution ($\nu = 1.9 \times 10^{-6}$ m^2 s^{-1}) in a vertical tube with (a) 22 mm—●, ○; (b) 32 mm—■, □; and (c) 52 mm—▲, △ internal diameter. The open symbols correspond to experiments with the laser diodes/photocells technique.

starts at the expected value of $Re_{U_L} \approx 2100$ for the transition of the liquid flow regime. This conclusion is valid for the three different column diameters used in the experiments.

Similar experiments with dilute to moderate aqueous glycerol solutions (1.9×10^{-6} m^2 s^{-1}, 4.2×10^{-6} m^2 s^{-1} and 5.7×10^{-6} m^2 s^{-1} kinematic viscosities) were performed in the vertical columns and they gave unexpected results as it is put in evidence in Figure 3(a)–(c) and Figure 4(a)–(d). Similar plots of Figure 2 are represented in Figure 3 for experiments with the less viscous solution (1.9×10^{-6} m^2 s^{-1}). It is apparent that the transition in the bubble velocity starts before the expected value of Re_{U_L}. The same conclusion is evident from Figure 4 where the experimental values of C are plotted against Re_{U_L}, for all the liquid viscosities. Once more the full and the open symbols correspond to data obtained with the pressure transducers and the diode-photocells, respectively, and the accordance between the two types of results is again very good. For the glycerol solutions, the transition in C (or in the bubble velocity) starts before the classical value $Re_{U_L} = 2100$, occurring for decreasing values of Re_{U_L} as the viscosity of the glycerol solution increases. For almost all the conducted experiments, the conditions observed $N_f > 300$ and $N_f^{4/3} M^{1/3} > 100$ were observed, the exceptions are some of the experiments carried out in the column with 22 mm of internal diameter where $N_f^{4/3} M^{1/3}$, for the worst conditions (water), is 66.

Complementary experiments were carried out to explain this unexpected behaviour. Two kinds of experiments were performed:

- The velocity of individual Taylor bubbles rising through water in the 32 mm acrylic column was measured at two distances from the gas injection, for a wide range of operating conditions. The pressure taps were, respectively at 4.0 m and 6.0 m from the gas injection. Similar values were obtained, for the same operating condition, suggesting that no entrance effects were felt, even at the lower distance from the gas entrance.
- Measurements of the velocity field in the flowing liquid ahead of the bubble nose were performed, at 6.0 m from the bottom of the 32 mm acrylic column, by means of a simultaneous PIV and shadowgraphy technique described by Nogueira *et al.* (2003). The results are shown in Figures 5(a) and (b), 6(a) and (b) and 7(a) and (b) for two aqueous glycerol solutions (solution A—$\nu = 1.9 \times 10^{-6}$ m^2 s^{-1}, $Re_{U_L} = 300$, $U_L/U_\infty = 0.09$, $We_{U_\infty} = 18.5$ and solution B—$\nu = 4.2 \times 10^{-6}$ m^2 s^{-1}, $Re_{U_L} = 1410$,

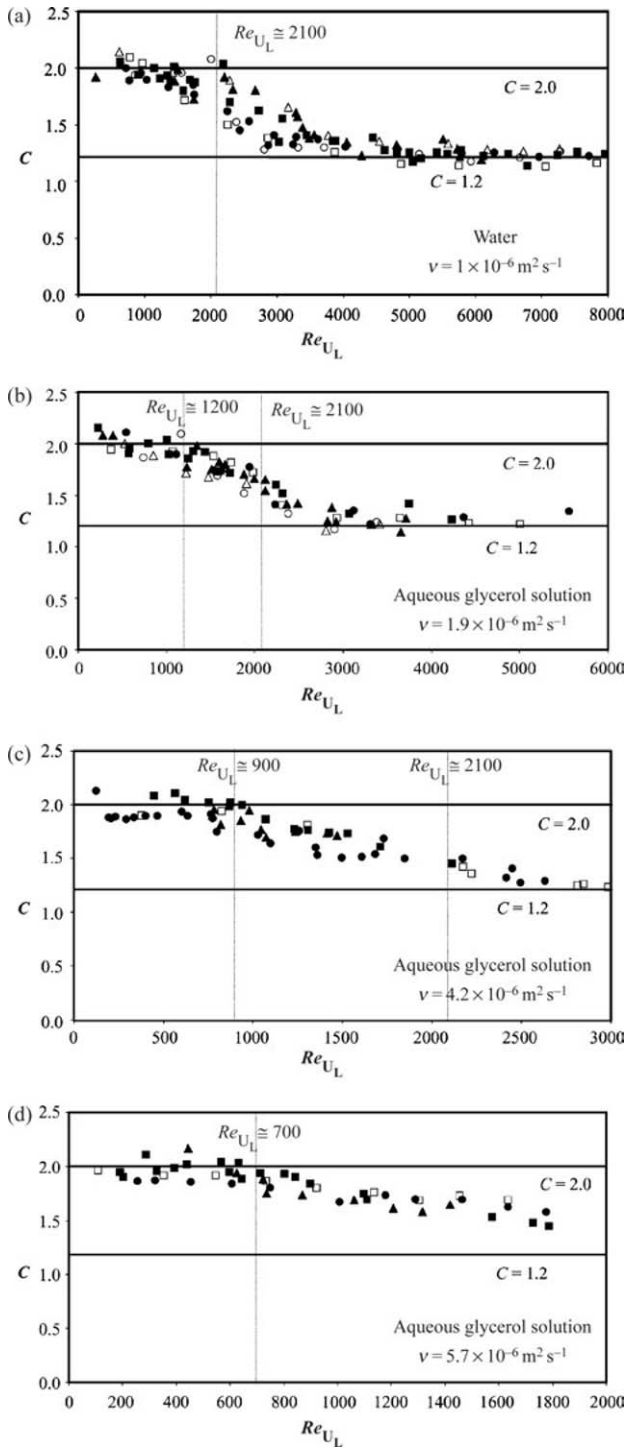

Figure 4. Experimental values of the coefficient velocity C as a function of Re_{U_L} obtained in the three columns for (a) water; (b) $\nu = 1.9 \times 10^{-6}\ m^2\ s^{-1}$; (c) $\nu = 4.2 \times 10^{-6}\ m^2\ s^{-1}$; (d) $\nu = 5.7 \times 10^{-6}\ m^2\ s^{-1}$. In the three plots, the symbols ●, ○, ■, □, and ▲, △ correspond to experiments performed in vertical tubes with 22 mm, 32 mm and 52 mm internal diameter, respectively. The open symbols correspond to experiments with the laser diodes/photocells technique.

$U_L/U_\infty = 0.90$, $We_{U_\infty} = 19.5$). Figure 5(a) and (b) represent the liquid velocity fields ahead of the Taylor bubbles in a fixed frame of reference. The axial coordinate z is taken relative to the nose of the bubble (positive downwards). The shape of the bubbles, simultaneously determined, is also represented. As depicted in the figures, the gas slug displaces the liquid ahead of it and the vectors near the interface slightly below the nose show a strong radial component. The presence of the bubble is also felt above the nose. This is well brought out in Figure 6(a) and (b) showing the evolution of the instantaneous velocity profiles along the axial distance from the nose. For the conditions studied, a dimensionless distance of $z/D \approx 0.6$ and $z/D \approx 0.8$ respectively, is needed for recovery of the laminar velocity profile. Finally, in Figure 7(a) and (b) the mean stabilized and dimensionless velocity profile ahead of the nose is plotted together with the undisturbed laminar profile. In both cases, the velocity profile is a well developed laminar profile.

The values obtained for the velocity coefficient from equation (1), as $C = (U - U_\infty)/U_L$, were $C = 1.90$ for solution A and $C = 1.60$ for solution B, with the bubble velocity determined from the diodes-photocells technique. Once more, a transition in the bubble velocity seems to occur before the expected value of Re_{U_L}, and more important than this, the regime ahead of the bubble nose is, as shown by these experiments, a developed laminar one.

In view of the unexpected results, it seems that the bubble velocity (or the coefficient C) experiences a transition, which is not a unique function of the liquid Reynolds number. Following this idea, a dimensional analysis was applied to the situation under study.

The bubble velocity is dependent of the liquid properties, ρ, σ, μ, diameter of the column, D, bubble velocity in the stagnant liquid, U_∞ and mean liquid velocity, U_L. It is also a function of the acceleration of gravity, g, through U_∞.

From dimensional analysis it follows that the bubble velocity, or C, is a function of Reynolds number of the liquid ($Re_{U_L} = DU_L/\nu$), Weber number for the bubble in a stagnant fluid ($We_{U_\infty} = \rho D U_\infty^2/\sigma$) and velocity ratio U_L/U_∞. For inertial controlled regime, $U_\infty = 0.35\sqrt{gD}$ and thus,

$$C = f'\left[\left(\frac{DU_L}{\nu}\right)^a \left(\frac{\rho(0{,}35\sqrt{g})^2 D^2}{\sigma}\right)^b \left(\frac{U_L}{(0.35\sqrt{g})D^{1/2}}\right)^c\right] \tag{5}$$

or

$$C = f\left[\left(\frac{DU_L}{\nu}\right)^a \left(\frac{\rho D^2}{\sigma}\right)^b \left(\frac{U_L}{D^{1/2}}\right)^c\right] \tag{6}$$

where a, b and c are constants and f and f' are unknown functions.

From Figures 4 (a)–(d) it is possible to observe that for a specific liquid (water or diluted to moderated aqueous glycerol solutions) the value of C is nearly the same for equal values of Re_{U_L} in the three different columns used in this study. This observation suggests that, for a given liquid, the value of C is a unique function of the product $U_L D$. Therefore, from equation (6), it can be concluded that C must be equal to $4b/3$ (since $a + 2b - 1/2c = a + c$). Equation (6) is then rewritten as

$$C = f\left[\left(\frac{1}{\nu}\right)^a \left(\frac{\rho}{\sigma}\right)^b (U_L)^{(a+4b/3)} (D)^{(a+4b/3)}\right] \tag{7}$$

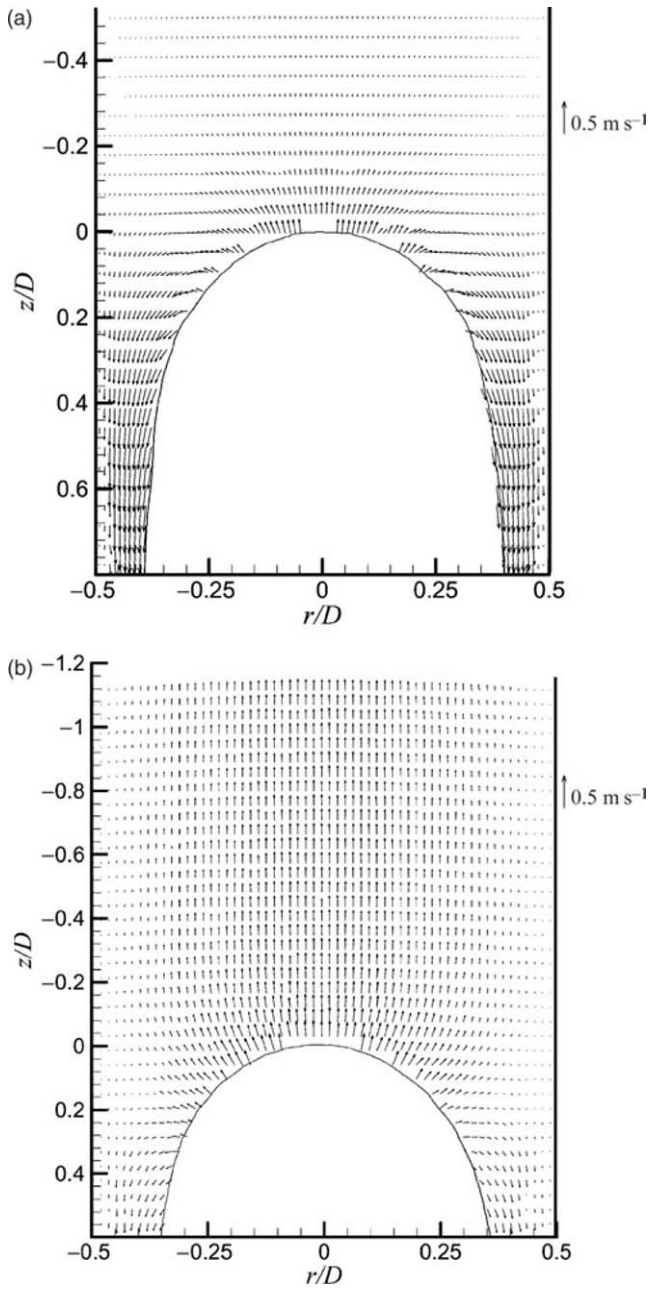

Figure 5. Representation of the liquid velocity fields ahead of the Taylor bubble in a fixed frame of reference for (a) solution A—$\nu = 1.9 \times 10^{-6}\,\mathrm{m^2\,s^{-1}}$, $Re_{U_L} = 300$, $U_L/U_\infty = 0.09$, $We_{U_\infty} = 18.5$; and (b) solution B—$\nu = 4.2 \times 10^{-6}\,\mathrm{m^2\,s^{-1}}$, $Re_{U_L} = 1410$, $U_L/U_\infty = 0.90$, $We_{U_\infty} = 19.5$.

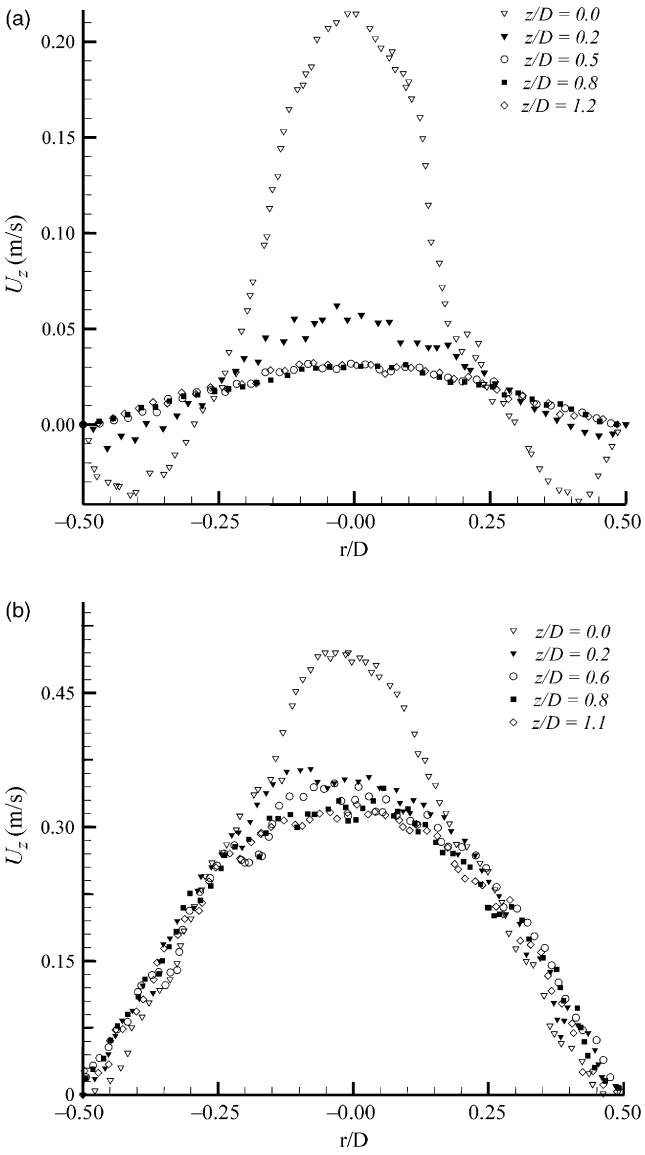

Figure 6. Evolution of the instantaneous velocity profiles along the axial distance from the nose of the Taylor bubble for (a) solution A—$\nu = 1.9 \times 10^{-6}\,\mathrm{m^2\,s^{-1}}$, $Re_{U_L} = 300$, $U_L/U_\infty = 0.09$, $We_{U_\infty} = 18.5$; and (b) solution B—$\nu = 4.2 \times 10^{-6}\,\mathrm{m^2\,s^{-1}}$, $Re_{U_L} = 1410$, $U_L/U_\infty = 0.90$, $We_{U_\infty} = 19.5$.

An estimate for the exponents a and b (or a and c) was obtained by processing the data for each column.

The experimental values of C are represented in Figure 8(a)–(c), for each column, as a function of $\nu^{-a}(\rho/\sigma)^b U_L^{(a+4b/3)}$. An optimization code (based on the Quasi-Newton method) was applied to obtain, for each column in the transition region, the pair of values a and b that minimize the root mean square deviation between the fitted function and the experimental data. The values found for each exponent do not differ much from column to column as shown in the abscissas represented in Figure 9(a)–(c).

Taking the mean values of the exponents (from the three columns), all the experimental values of C are plotted as a function of $Re_{U_L}^a We_{U_\infty}^b (U_L/U_\infty)^c$ in Figure 9. A functional dependence between the dimensionless numbers is evident from this plot. The functionality is the following:

$$C = 2.0 \pm 0.1 \quad \text{for } Re_{U_L} We_{U_\infty}^{0.21} (U_L/U_\infty)^{0.28} < 1000$$

$$C = 2.08 - 0.000138 Re_{U_L} We_{U_\infty}^{0.21} (U_L/U_\infty)^{0.28};$$

$$1000 < Re_{U_L} We_{U_\infty}^{0.21} (U_L/U_\infty)^{0.28} < 6000$$

$$C = 1.2 \pm 0.1 \quad \text{for } Re_{U_L} We_{U_\infty}^{0.21} (U_L/U_\infty)^{0.28} > 6000$$

In Figure 9 the error bars in some experimental data are drawn considering an error of 3% in the measured variables U and U_L. The linear correlation fitted in the transition region is, for almost all the data, inside the error bands.

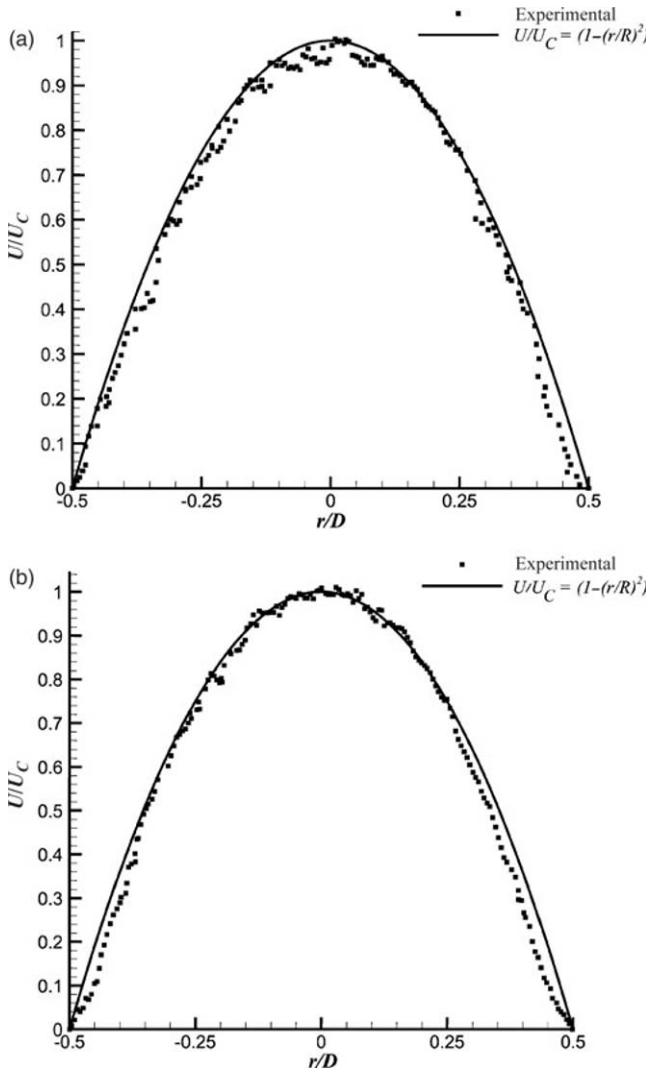

Figure 7. Comparison of the mean stabilized velocity profile ahead of the Taylor bubble with the theoretical parabolic profile for laminar regime in the liquid for (a) solution A—$\nu = 1.9 \times 10^{-6}$ m^2 s^{-1}, $Re_{U_L} = 300$, $U_L/U_\infty = 0.09$, $We_{U_\infty} = 18.5$; and (b) solution B—$\nu = 4.2 \times 10^{-6}$ m^2 s^{-1}, $Re_{U_L} = 1410$, $U_L/U_\infty = 0.90$, $We_{U_\infty} = 19.5$.

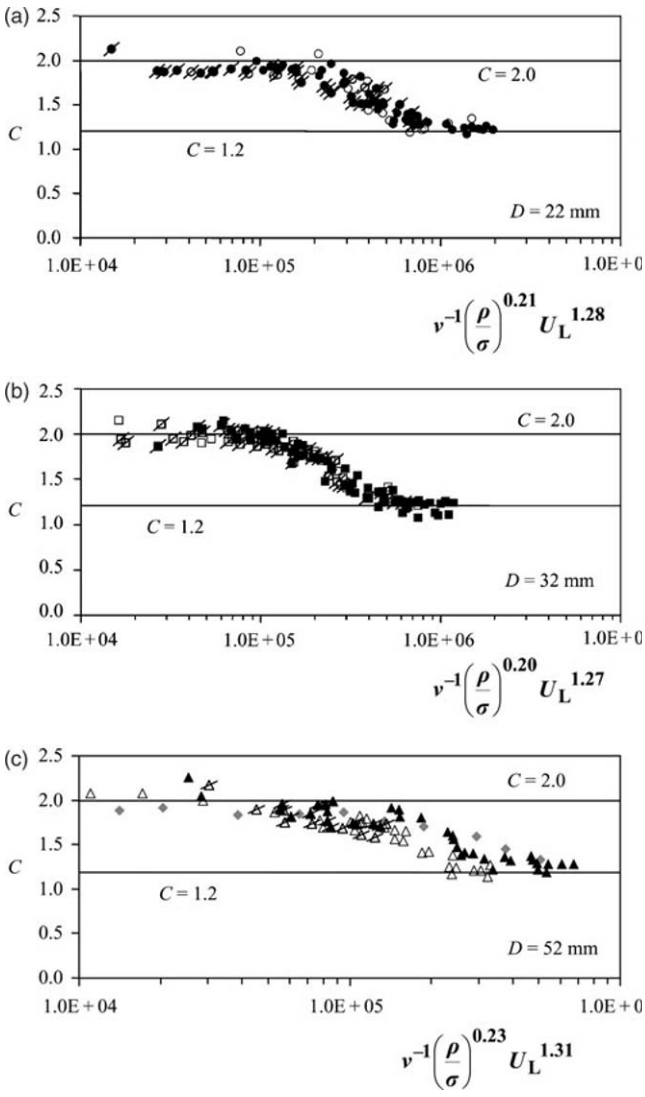

Figure 8. Experimental values of the coefficient velocity C as a function of $\nu^{-a}(\rho/\sigma)^b U_L^{(a+4/3b)}$ for all the liquid viscosities obtained in a vertical tube with (a) 22 mm, (b) 32 mm and (c) 52 mm internal diameter. In the three plots the full symbols correspond to experiments with water, the open symbols with a glycerol solution $\nu = 1.9 \times 10^{-6}$ m^2 s^{-1}, the full-dashed symbols with a glycerol solution $\nu = 4.2 \times 10^{-6}$ m^2 s^{-1}; and the open-dashed symbols with a glycerol solution $\nu = 5.7 \times 10^{-6}$ m^2 s^{-1}. In the plot 6(c) the symbol ◆ corresponds to data obtained by Collins *et al.* (1978).

In Figures 8(c) and 9 the experimental data obtained by Collins *et al.* (1978) are also represented. One of the objectives of the experiments carried out by the authors was to measure the Taylor bubble velocity in the laminar region ($0 < Re_{U_L} < 2100$) and in the transition region ($2100 < Re_{U_L} < 4000$) in inertial controlled regime. The authors met these conditions with a 48% glycerol–water mixture in a column with 51.4 mm of internal diameter ($N_f = 7600$ and $N_f^{4/3}M^{1/3} \approx 420$). The column was 4.0 m long and the measuring section was located 2.5 m above the air injection. The deviation of the experimental points from the predictions [equation (4)], in the range $760 < Re_{U_L} < 2100$ was, according to the authors, caused by entrance effects, being the laminar profile in the liquid fully developed only at low Re_{U_L} numbers (<760). The data of Collins *et al.* (1978) are in reasonable agreement with the correlation found for the transition region and therefore the entrance effects are not an accurate justification.

Also, the explanation suggested by Fréchou (1986) and Mao and Dukler (1991) for their unexpected results of C as a function of Re_{U_L} numbers for a train of bubbles is not adequate since similar results were obtained in the present work with individual bubbles rising in a co-current flowing liquid.

In the present paper, a useful correlation is given to calculate the Taylor bubble velocity rising in a vertical tube in a co-current flowing liquid. It seems that the transition in the velocity (through the variations in coefficient C) starts even when the flow regime in the liquid ahead of the bubble is still laminar. However, the physical justifications for such behaviour are not clear.

For all the performed experiments, the flow in the wake of bubble was turbulent with some vortice structures and continuous oscillation of the bubble bottom. These oscillations induce an unsteady pressure field in the bubble bottom with direct consequences on the drag forces

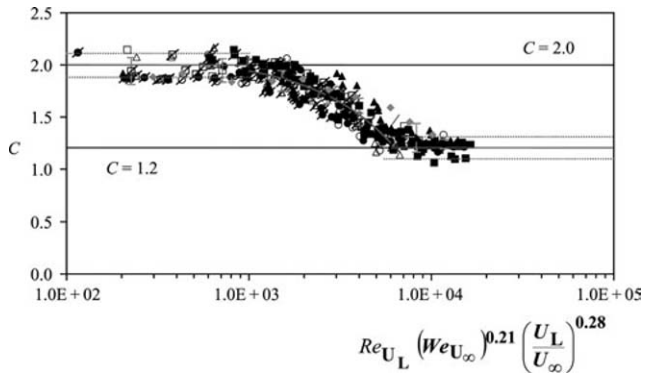

Figure 9. Experimental values of the velocity coefficient C versus $Re_{U_L}^{a} We_{U_\infty}^{b} (U_L/U_\infty)^{c}$ for the entire range of operation conditions and representation of the fitted function. The symbol ◆ corresponds to data obtained by Collins *et al.* (1978).

experienced by the bubble. Since the shape of the bubble nose and the distance needed to have a stabilized liquid film flowing around the bubble, strongly depend on U_L/U_∞ and We_{U_∞} only a detailed analysis of the forces along the bubble interface, in particular at the bubble nose and bottom, can shed new light to the interpretation of the obtained results.

The results reported in the present work are important to the simulation of two-phase vertical slug flow mainly in small to moderate pipe diameters, with liquids of low to moderate viscosities. Important applications are, e.g., the air-lift bio-reactors where the selection of operating conditions with high values of gas hold-up enhances mass transfer processes. This favourable situation can occur for conditions identified in the present work, corresponding to a bubble velocity lower than expected for laminar flow regime, as was also found by Coelho Pinheiro *et al.* (2000) for aerated slugging columns.

CONCLUSIONS

An experimental study on the transition in the Taylor bubble velocity in vertical upward two-phase slug flow is presented. Values for the velocity of isolated bubbles were determined in a wide range of operating conditions, corresponding to the inertial controlled regime. The bubble velocities were measured at a sufficiently high distance from the injection region to eliminate entrance effects.

The results obtained showed that for aqueous glycerol solutions with low to moderate viscosities, the bubble velocity experiences a transition at different values of Re_{U_L}, which means that C is not an unique function of Re_{U_L}.

A general empirical correlation was established to predict the velocity coefficient C as a function of Re_{U_L}, U_L/U_∞ and We_{U_∞}.

These results are very important in the modelling of two-phase slug flow since successful models rest strongly on the understanding of the Taylor bubble motion.

NOMENCLATURE

a,b,c	exponents in equation (5)
C	velocity coefficient
D	internal column diameter, m
f, f'	function
Fr	Froude number $(=U_\infty/(gD)^{1/2})$
g	acceleration due to gravity, m s^{-2}
M	Morton number $(=g\mu^4/\rho\sigma^3)$
N_f	dimensionless parameter $(=g^{1/2}D^{3/2}/\nu)$
r	radial distance, m
R	column radius, m
Re_{U_L}	Reynolds number for the liquid $(=DU_L/\nu)$
U	Taylor bubble velocity, m s^{-1}
U_C	liquid velocity at the column axis, m s^{-1}
U_L	liquid superficial velocity in the column, m s^{-1}
U_∞	velocity of an individual bubble rising in a stagnant liquid, m s^{-1}
We_{U_∞}	Weber number for the bubble in a stagnant fluid $(=\rho U_\infty^2 D/\sigma)$
z	axial coordinate, m

Greek symbols

σ	liquid surface tension, N m^{-1}
ν	liquid kinematic viscosity, m^2 s^{-1}
ρ	liquid density, kg m^{-3}
ϕ	functional relationship
μ	liquid viscosity, Pa s

REFERENCES

Campos, J.B.L.M. and Guedes de Carvalho, J.R.F., 1988, An experimental study of the wake of gas slugs rising in liquids, *J Fluid Mech*, 196: 27–37.

Coelho Pinheiro, M.N., Pinto A.M.F.R. and Campos J.B.L.M., 2000, Gas hold-up in aereated slugging columns, *IChemE Trans, Part A, Chem Eng Res Design*, 78: 1139–1146.

Collins, R., De Moraes, F.F., Davidson, J.F. and Harrison, D., 1978, The motion of a large gas bubble rising through liquid flowing in a tube, *J Fluid Mech*, 89: 497–514.

Fabre J. and Liné A., 1992, Modeling of two-phase slug flow, *Ann Rev Fluid Mech*, 24: 21–46.

Fréchou, D., 1986, Étude de L'ecoulement ascendant à trois fluides en conduite verticale, Thèse Inst Natl Polythech, Toulouse, France.

Govier, G.W. and Aziz, K., 1972, *The Flow of Complex Mixtures in Pipes*, 388–414 (Van Nostrand, New York, USA).

Mao, Z.-S. and Dukler, A., 1991, The motion of Taylor bubbles in vertical tubes. II—Experimental data and simulations for laminar and turbulent flow, *Chem Eng Sci*, 46: 2055–2064.

Nicklin, D.J., Wilkes, J.O. and Davidson, J.F., 1962, Two-phase flow in vertical tubes, *Trans IChemE*, 40: 61–68.

Nogueira, S., Sousa, R.G., Pinto, A.M.F.R., Riethmuller, M.L. and Campos, J.B.L.M., 2003, Simultaneous PIV and pulsed shadow technique in slug flow: a solution for optical problems, *Exp in Fluids*, 35: 598–609.

Pinto, A.M.F.R. and Campos, J.B.L.M., 1996, Coalescence of two gas slugs rising in a vertical column of liquid, *Chem Eng Sci*, 51: 45–54.

Pinto, A.M.F.R., Coelho Pinheiro, M.N. and Campos, J.B.L.M., 1998, Coalescence of two gas slugs rising in a co-current flowing liquid in vertical tubes, *Chem Eng Sci*, 53: 2973–2983.

Polonsky, S., Barnea, D. and Shemer, L., 1998, Image processing procedure for analyzing the motion of an elongated bubble rising in a vertical pipe, *Proc 8th International Symposium on Flow Visualization*, 117.1–117.10, Sorento Italy.

Stewart, P.S.B. and Davidson, J.F., 1967, Slug flow in fluidised beds, *Powder Technol*, 1: 61–80.

White, F.M., 1974, *Viscous Fluid Flow*, 388 (McGraw-Hill, New York, USA).

White E.T. and Beardmore, R.H., 1962, The velocity of rise of single cylindrical air bubbles through liquids contained in vertical tubes, *Chem Eng Sci*, 17: 351–361.

Zukoski, E.E., 1966, Influence of viscosity, surface tension and inclination angle on motion of long bubbles in closed tubes, *J Fluid Mech*, 25: 821–837.

ACKNOWLEDGEMENTS

The partial support of 'Fundação para a Ciência e Tecnologia—Portugal' through project POCTI/EQU/33761/1999 is gratefully acknowledged: POCTI (FEDER) also supported this work via CEFT.